

## DISCRETE PROBABILISTIC MODEL OF BED-LOAD LAYER AS GRANULAR ASSEMBLES

By

Hitoshi GOTOH

Lecturer, Department of Civil Engineering, Kyoto University  
Yoshida Honmachi, Sakyo-ku, Kyoto, 606, Japan

Tetsuro TSUJIMOTO

Associate Professor, Department of Civil Engineering, Kanazawa University  
2-40-20, Kodatsuno, Kanazawa, 920, Japan

and

Hiroji NAKAGAWA

Professor, Department of Civil and Environmental Systems Engineering, Ritsumeikan University  
1916, Noji-cho, Kusatsu-shi, Shiga, 525, Japan

### ABSTRACT

Discrete probabilistic model of the motion of saltating particles is proposed to investigate the structure of the bed-load layer in detail. Motion of the multiple saltating particles are traced by the stochastic simulation based on the Lagrangian model by considering the interparticle collision and the irregularity of the collision and repulsion at the bed surface. The instantaneous motions of saltating particles are displayed as a series of snapshots of simulation, and the existing height distribution and the velocity profile of moving particles are predicted. The clear discrepancies are found out between the results of the present simulation and that of the simulation in which the motion of the single particle is traced without considering the interparticle collision. This fact demonstrates an important role of the interparticle collision in the bed-load layer.

### INTRODUCTION

The fundamental characteristic of the bed-load motion is its irregularity due to collision and repulsion at the bed-surface and the interparticle collisions. The stochastic model is the one of the most effective methods to express this characteristic, because it can describe the probabilistic varieties of the particle/bed-materials and particle/particle collisions. Tsujimoto and Nakagawa (1) performed the stochastic simulation of successive saltation with the two-dimensional hypothetical repulsive plane which expresses the irregularity of the collision at the bed-surface. Tohdoh, Sekine and Kikkawa (2) executed numerical simulation of successive saltation about the same period with Tsujimoto and Nakagawa. Wiberg and Smith (3) also executed the numerical simulation of the saltation in flowing water. Sekine and Kikkawa (4) extended their simulation model to the three-dimensional plane, and found that the transverse motion of the bed-load particle is so small that it can be disregarded as compared to that in the streamwise and upward-vertical directions.

The other essential characteristics of bed-load transport is the existence of the bed-load layer: the high concentration of sediment is transported within the thin layer in the vicinity of the bed surface. Such confinement of the moving region of bed-load particle makes the following two kinds of interactions dominant: (i) particle/flow (solid/liquid) interaction and (ii) interparticle collision.

One of the most suggestive approaches for describing the former interaction is the PSI-cell model proposed by Crowe, Sharma and Stock (5). Nakagawa, Tsujimoto and Gotoh (6) proposed a simulation model of the saltation layer by introducing PSI-cell model for the coupling of the solid (particle) and liquid (flow) phases.

The latter interaction is too complicated to be investigated experimentally even by the present measuring techniques. Hence the numerical simulation of the granular assemblies is a trump for overcoming the deficiency of the experiment in clarifying the interparticle collision. The most popular approach to the interparticle collision is the Distinct Element Method (DEM) proposed by Cundall and Strack (7). DEM is originally proposed as an effective approach to the situation that each constitutive element gathers closer and the deformation of the medium is sufficiently small. In the bed-load layer, however, the motion of particle is very rapid and the relative position of the individual particle also changes rapidly. A suggestive method to the rapid motion of the particles was proposed by Campbell and Brennen (8) for simulating the steady granular shear flow. Each element is connected by the spring and dashpot for describing the interaction among the contacted particles in DEM; while in Campbell and Brennen's model a straight-forward approach to the interparticle relation was intended based on the classical dynamics of rigid body.

DEM is applicable to the simultaneous contact of multiple particles; while, in Campbell and Brennen's model, each particle should not collide with more than two particles during the time step of the calculation. Hence, under the high concentration of the sediment, Campbell and Brennen's model requires very short time step of the calculation and it prevents the computational efficiency. Meguro, Iwashita and Hakuno (9) performed the simulation of the debris flow by the DEM in which some parts of the calculation of the contacting force among the constitutive elements are modified by considering the momentum conservation law. The advantage of the DEM is the applicability to the various situations; while the advantage of Campbell and Brennen's model is the exact treatment of the interparticle collision.

In this study, the successive saltation model proposed by Tsujimoto and Nakagawa (1) is combined with the Campbell and Brennen's model for interparticle collision, in other words, Lagrangian model of the saltating particles is extended to describe the motion of multiple particles simultaneously. Although the authors have already proposed a simulation model for the particle/flow interaction in bed-load layer (6), particle/flow interaction is not here considered in order to simplify the problems and to clarify the purpose of this study. Hence the clear water assumption in which the log-law of flow-velocity distribution is supposed is applied to flow field.

## SIMULATION MODEL

### *General Feature of present simulation*

In the stochastic simulation of successive saltation, we estimate the characteristics of the saltating particles as the long-time average of the irregular motion of single saltating particle. In such an approach, we cannot trace the trajectories of multiple particles simultaneously, consequently the interparticle collision cannot be strictly considered. This deficiency of the stochastic simulation has been prevented the application of probabilistic analysis to the bed-load transport under the high-bed shear stress, where the interparticle collision occurs frequently. In this paper, the previous simulation model of successive saltation is refined to be able to trace the multiple saltating particles simultaneously in special regards to the interparticle collision.

In the uni-directional uniform streams, the streamwise components of flow- and particle-velocity are dominant, and the vertical component of particle velocity is also dominant due to the collision and repulsion at the bed-surface. Therefore, for the simplicity, the streamwise and vertical two-dimensional motion of the saltating spherical particles are traced in the domain between two vertical planes which stand each other at the interval of particle's diameter, as shown schematically in Fig. 1. The definition sketch of the calculating domain is shown in Fig. 2. For the simplicity, the steady and uniform flow, in the inclined channel with the angle  $\theta$  to the horizontal direction, is treated in this study, therefore the periodic boundary condition is applied at the upstream and downstream boundaries, the detail of which is mentioned later.

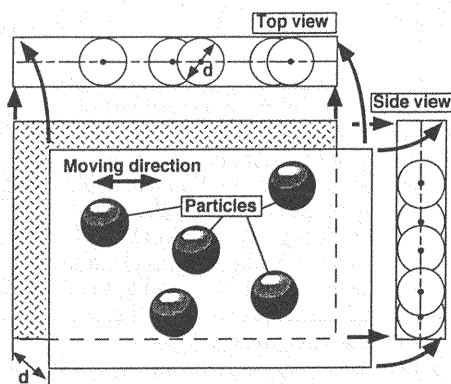


Fig. 1 Two-dimensional motion of saltating particles

### Motion of Individual Particle

Motion of an individual saltating particle is not so keenly affected by the flow-turbulence that the moving process of the particle apart from a bed surface can be regarded as the deterministic process; while the collision and repulsion at an irregular bed surface bring the stochastic characteristics of the saltation. Hence the key of the saltation model is how to describe an irregular collision at a bed surface. The body of studies (Tsujiimoto and Nakagawa (1); Tohdoh, Sekine and Kikkawa (2); Wiberg and Smith (3); and Sekine and Kikkawa (4)) were performed to describe the irregular motion of the saltating particle due to the collision and repulsion at a bed surface. In this study, the simulation model of the irregular successive saltation with the two-dimensional hypothetical repulsive plane, which was proposed by Tsujiimoto and Nakagawa (1), is modified and generalized.

The trajectory of the saltation is governed by the following equations.

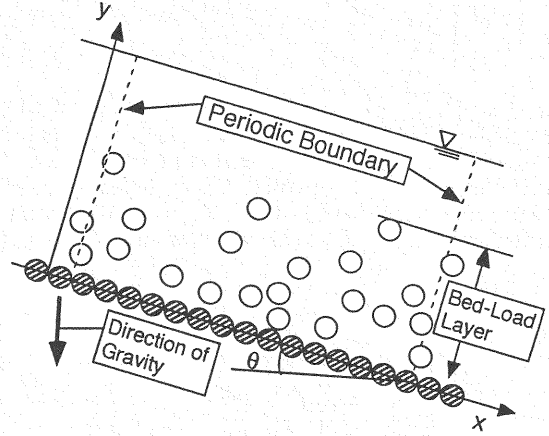


Fig. 2 Definition sketch of calculating domain

$$\rho \left( \frac{\sigma}{\rho} + C_M \right) A_3 d^3 \frac{du_p}{dt} = \frac{1}{2} C_D \rho A_2 d^2 \sqrt{(U - u_p)^2 + (V - v_p)^2} (U - u_p) \quad (1)$$

$$\rho \left( \frac{\sigma}{\rho} + C_M \right) A_3 d^3 \frac{dv_p}{dt} = \frac{1}{2} C_D \rho A_2 d^2 \sqrt{(U - u_p)^2 + (V - v_p)^2} (V - v_p) - \rho \left( \frac{\sigma}{\rho} - 1 \right) g A_3 d^3 \quad (2)$$

$$C_D = C_{D\infty} + \frac{24}{Re} ; \quad Re = \frac{d \sqrt{(U - u_p)^2 + (V - v_p)^2}}{\nu} \quad (3)$$

where  $x, y$  = the streamwise and upward vertical coordinates, respectively;  $U, V$  = mean velocity components in  $x, y$  directions, respectively;  $\rho$  = mass density of fluid;  $g$  = gravitational acceleration;  $d$  = diameter of saltating particle;  $u_p, v_p$  = streamwise and upward vertical components of speed of the saltating particle, respectively;  $C_M$  = added mass coefficient (=0.5);  $\sigma$  = mass density of saltating particle;  $A_2, A_3$  = two- and three-dimensional geometrical coefficients of particle ( $A_2 = \pi/4, A_3 = \pi/6$ ), respectively; and  $C_D$  = drag coefficient. The parameter  $C_{D\infty}$  depends on the shape of the particle:  $C_{D\infty} = 0.4$  for a sphere; and  $C_{D\infty} = 2.0$  for the natural sand as recommended by Rubey (10). The turbulence of flow velocity is neglected in the equation of motion, because the previous experimental results (Tsuchiya and Aoyama (11); Nakagawa, Tsujiimoto and Akao (12)) indicate that the trajectory of saltation is not keenly affected by the turbulence.

### Collision and repulsion at bed surface

The bed surface is assumed to be composed by the spherical particles which have the same diameter as the saltating particles. The bed material particles are to be densely arranged, the centroids of which are located on the same elevation as shown in Fig. 2. All of the coordinates of bed material particles are calculated before the beginning of the simulation of saltations, and they are stored in the memories to be referred in the collision assessment of saltating particles.

Even if all of the bed-material particles exposed at a surface are located at the same elevation, the collision and repulsion are not deterministic because of the irregularity of a colliding point due to the geometry of a bed-material particle. In this simulation the bed-material particle is spherical, therefore the geometrical characteristics is represented by the angle of hypothetical repulsing plane against the mean bed surface,  $\alpha$ . Fig. 3 shows a definition sketch of the collision and repulsion. The change in the speed of a saltating particle by collision and repulsion on a bed surface is written as follows:

$$\begin{bmatrix} u_{gout} \\ v_{gout} \end{bmatrix} = \Xi_0 \cdot \begin{bmatrix} u_{gin} \\ v_{gin} \end{bmatrix} ; \quad \Xi_0 = \begin{bmatrix} e \cdot \cos^2 \alpha - f \cdot \sin^2 \alpha & (e + f) \cos \alpha \sin \alpha \\ (e + f) \cos \alpha \sin \alpha & e \cdot \sin^2 \alpha - f \cdot \cos^2 \alpha \end{bmatrix} \quad (4)$$

where  $(u_{gin}, v_{gin}), (u_{gout}, v_{gout})$ =velocity vectors of saltating particle just before and after the collision, respectively; and  $e, f$ =repulsive coefficients. The angel  $\alpha$  distributes in a certain range. Fig. 4 shows the extreme situation of the distributing range of  $\alpha$ . The saltating particle B collides with the bed material particle A. The particle A is sheltered by the particle C when the angle between the depositing direction and the mean bed surface,  $\theta_{in}$ , is smaller than  $\pi/6$ . The angle  $\alpha$  is formulated as a function of  $\theta_{in}$  after some geometrical considerations as follows:

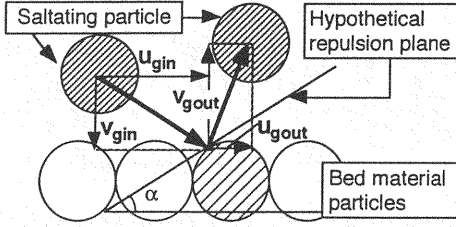


Fig. 3 Definition sketch of collision and repulsion at a bed-surface

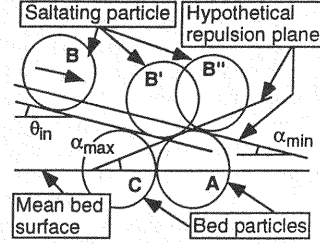


Fig. 4 Maximum and minimum  $\alpha$

$$\alpha = \begin{cases} \text{Arcsin}\{(1 - \xi_0) \sin \theta_{in} - 1\} - \theta_{in} + \frac{\pi}{2} & \text{for } \theta_{in} \leq \frac{\pi}{6} \\ \text{Arcsin}\left\{\left(\frac{1}{2} - \xi_0\right) \sin \theta_{in} - \frac{\sqrt{3}}{2} \cos \theta_{in}\right\} - \theta_{in} + \frac{\pi}{2} & \text{for } \theta_{in} > \frac{\pi}{6} \end{cases} \quad (5)$$

The condition of successive saltation at a bed is given by the following equation.

$$\left(\frac{\sigma}{\rho} + C_M\right) \frac{v_{out}^2}{2} > \left(\frac{\sigma}{\rho} - 1\right) g \Delta_b \quad (6)$$

where  $\Delta_b$ =height of a protruding obstruction on a bed due to the irregularity of bed surface ( $\Delta_b/d=0.1$  in this study). This equation implies that the kinetic energy of the vertical velocity of a saltating particle just after collision is smaller than the potential energy of a protruding obstructions.

### Interparticle Collision

Two particles are taken to be in contact, when the distance between their centers  $((x_i, y_i), (x_j, y_j))$  is less than the sum of their radii as follows:

$$\sqrt{(x_i - x_j)^2 + (y_i - y_j)^2} < d \quad (7)$$

This condition is assessed at every time step of calculation after updating the position of particles, and if this condition is satisfied, the point of contact is determined by the following manner as illustrated in Fig. 5 where  $i=1$  and  $j=2$ .  $(x_{bi}, y_{bi}), (x_{ai}, y_{ai})$  are the positions of particle  $i$  at  $t$  and  $t+\Delta t$ , respectively.  $(x_{ai}, y_{ai})$  is the virtual position at  $t+\Delta t$  for calculating the colliding point and Eq. 7 is to be satisfied at  $t+\Delta t$ . Introducing a linear approximation to the trajectories of saltation during  $\Delta t$  leads following equations.

$$y_i = \frac{y_{ai} - y_{bi}}{x_{ai} - x_{bi}}(x_i - x_{bi}) + y_{bi} \quad (i = 1, 2) \quad (8)$$

$$x_i = x_{bi} + (x_{ai} - x_{bi}) \cdot r_c \quad (i = 1, 2) \quad (9)$$

where  $r_c$ =ratio of division between the positions at  $t$  and  $t+\Delta t$ . At the colliding point, the distance between the centers of two particles  $((x_i, y_i), (x_j, y_j))$  is equal to the sum of their radii as follows:

$$\sqrt{(x_i - x_j)^2 + (y_i - y_j)^2} = d \quad ; \quad r_c \leq 1 \quad (10)$$

The ratio of division  $r_c$  is determined by solving Eq. 10 with Eqs. 8 and 9, and then the coordinate and the speed of the particle at the colliding point are calculated by using  $r_c$  and the linear interpolation.

The change in the particle's speed due to the collision is estimated by considering the common tangent to the both particles at the colliding point as similar as the hypothetical repulsive plane. The angle of the hypothetical repulsive plane against the streamwise direction  $\phi$  is given as follows:

$$\phi = \text{Arctan} \left( -\frac{x_{c1} - x_{c2}}{y_{c1} - y_{c2}} \right) \quad (11)$$

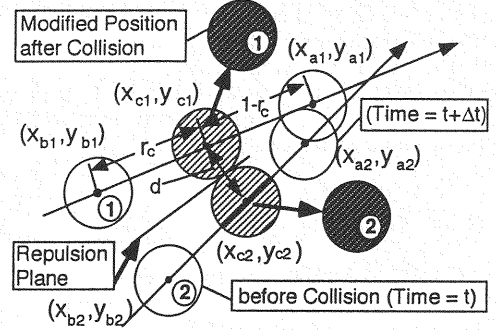


Fig. 5 Definition sketch of interparticle collision

where  $(x_{ci}, y_{ci})$ =centers of the colliding particles  $(i=1,2)$ . By considering the momentum conservation law and the law of repulsion in the directions parallel and vertical to the hypothetical repulsive plane, the speeds of the particles just before and just after a collision are related to each other as follows:

$$\begin{bmatrix} u_1^{out} \\ v_1^{out} \\ u_2^{out} \\ v_2^{out} \end{bmatrix} = \frac{1}{2} \begin{bmatrix} \xi_1 & \lambda & \xi_2 & -\lambda \\ \lambda & \xi_3 & -\lambda & \xi_4 \\ \xi_2 & -\lambda & \xi_1 & \lambda \\ -\lambda & \xi_4 & \lambda & \xi_3 \end{bmatrix} \begin{bmatrix} u_1^{in} \\ v_1^{in} \\ u_2^{in} \\ v_2^{in} \end{bmatrix} ; \quad \begin{cases} \xi_1 = (1 + e_p) \cos^2 \phi + (1 - f_p) \sin^2 \phi \\ \xi_2 = (1 - e_p) \cos^2 \phi + (1 + f_p) \sin^2 \phi \\ \xi_3 = (1 + e_p) \sin^2 \phi + (1 - f_p) \cos^2 \phi \\ \xi_4 = (1 - e_p) \sin^2 \phi + (1 + f_p) \cos^2 \phi \\ \lambda = (e_p + f_p) \cos \phi \sin \phi \end{cases} \quad (12)$$

where  $e_p, f_p$ =interparticle repulsive coefficients, and the subscripts “in” and “out” express the values before and after the collision, respectively.

### Periodic Boundary Condition

Since the uniform flow is treated in this study, the upstream and downstream sides of the control volume are bounded by the periodic boundaries, which improves a computational efficiency by limiting the number of the particles contained initially in the control volume. A particle passing through the one of the periodic boundaries reenters into the control volume immediately through the other periodic boundary.

In this calculation, some contrivance is required to satisfy the periodic boundary condition, because the motion of particles is not always downstream direction due to the interparticle collision with other moving particles. A particle which just passes out the downstream periodic boundary has a chance to collide with other particle to move in the upstream direction and it has a possibility to reenter the control volume through the downstream periodic boundary. In order to overcome this difficulty, the following technique is adopted here: The particles in the neighborhood of the periodic boundaries are duplicated as illustrated in Fig. 6. In other words, special regions named ‘duplicated particle region’ abbreviated “DPR” are prepared just neighboring downstream of the both boundary sides of the control volume. In Fig. 6, the shaded area is the control volume, and the areas surrounded by the dashed lines are DPR,

respectively. The dummy particles are introduced in the downstream DPR, and the motion of pairs of the particles in the upstream and downstream DPRs are synchronized with each other perfectly. Hence, if the particle in one DPR collides with the particle outside of the DPR, the effect of the collision is delivered to the particle in the other DPR in calculation. When a particle moves out of DPR, the dummy particle is deleted from a memory. By introducing the DPR, the periodic boundary condition is satisfied even under the existence of the particle which passes through the side boundaries in the upstream direction.

### Procedure of Simulation

Figure 7 shows the procedure of simulation as follows: [1] The individual saltation is traced to estimate the existing height and the velocity of the saltating particle in clear-water flow, or without an interparticle collision; [2] The initial positions and velocities of the particles are determined on the basis of the calculated results in clear-water flow. [3] The motion of particles during a time  $\Delta t$  are traced by integrating the Eqs. 1 and 2 numerically with taking account of the interparticle collision. [4] If the collisions occur during  $\Delta t$ , the position and the velocity of particle after a collision is calculated by the Eqs. 6~11, and they are updated. [5] This procedure is iterated during  $T_a$ , and the existing probability and the velocity of saltating particles at respective height are averaged in each  $T_a$  for judging the convergence of the simulation. The time for averaging  $T_a$  is set 1s in this simulation.

Table 1 shows the hydraulic condition of numerical simulation and flume experiment, where  $I_e$ =energy gradient;  $h$ =flow depth;  $U_m$ =bulk mean velocity;  $u_*$ =shear velocity; and  $\tau_*$ =dimensionless bed shear stress. Spherical glass beads of the specific gravity 2.60 and the diameter 0.4 cm are used as test particles in simulation and experiment. In this simulation the number of particles initially placed in the control volume is determined in a following manner: Firstly, the number of particles, which is not necessarily an integer, are calculated based on the Meyer-Peter and Müller's sediment transport formula (13) by supposing the length of the control volume in the streamwise direction. And then the length of the control volume in streamwise direction is adjusted with care to set the integer number of particles in it.

The motion of the particles are traced explicitly in this simulation, therefore the convergence and the stability of the simulation is keenly affected by the time step  $\Delta t$ . If the time step is set longer than an appropriate value, a saltating particle may collide twice with other

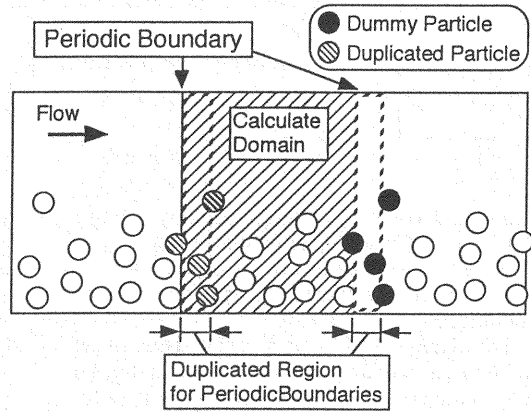


Fig. 6 Periodic boundary

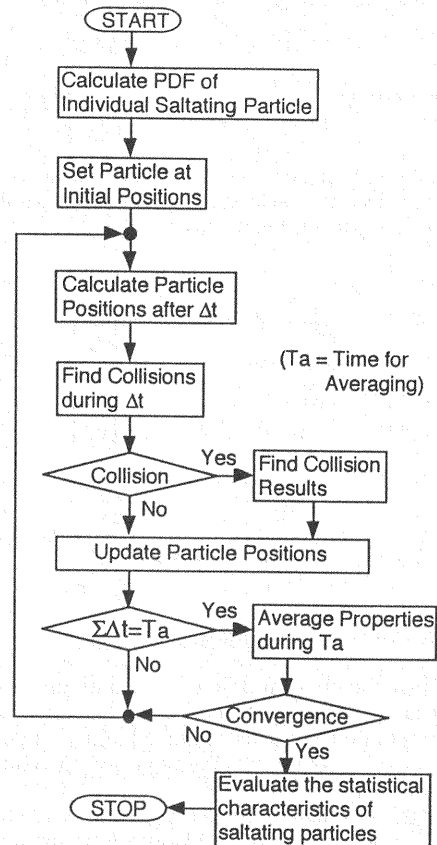


Fig. 7 Procedure of simulation

Table 1 Condition of experiment

$I_e$	$h(\text{cm})$	$U_m(\text{cm/s})$	$u_*(\text{cm/s})$	$\tau_*$
0.02	6.05	136.4	11.6	0.16

particles during  $\Delta t$ , then the multiple collision assessments are required for calculating the motion of single particle during  $\Delta t$  and, consequently the complicated computer algorithm is required. On the other hand, if the time step is set too shorter than an appropriate value, the simulation becomes time-consuming, or it takes long time to converge. In this simulation, the time step is set  $\Delta t=0.002$  s by a trial and error method to avoid the multiple collision assessments and the decline of computational efficiency.

## RESULTS AND DISCUSSIONS

### *Instantaneous motion of saltating particles*

This simulation provides a huge amount of data on the instantaneous motion of saltating particles, or their positions and velocities. Although our main purpose is to estimate the mean structure of saltation through the averaging operation of these data, the instantaneous motion of saltating particles is also important to understand the physical aspect of the phenomena. Furthermore, the reliability of the simulation is promoted by visualizing the instantaneous motion of the particles. Fig. 8 shows the typical snapshots of the continual 10 frames which show the results of the simulation after the convergence.

In Fig. 8, the momentum transport due to interparticle collision was detected among the particles Nos. 2, 5 and 6. In the frame C, the descending particle No. 6 and the ascending particle No. 2 collide with each other and repulse; and then the vertical component of both particle's velocity change the sign in the frame D: the particle No. 6 moves upward, and the particle No. 2 moves downward. In the frame E, the descending particle No. 2, which has lost its momentum due to the collision with the particle No. 6, collides with the ascending particle No. 5 and gains the upward vertical momentum. In the frame F, the descending particle No. 5, which has lost its momentum due to the collision with the particle No. 2, collides and repulses at the bed-surface, and then it moves upward. In the frame G, the particle No. 5 collides again with the particle

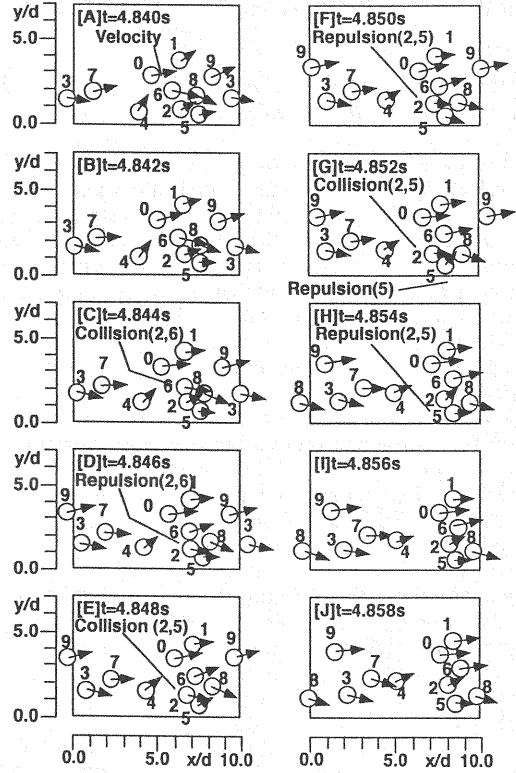


Fig. 8 Instantaneous motion of particles

No. 2 and supplies the momentum to the particle No. 2. Hence the upward momentum possessed of the particle No. 5, which moves in the vicinity of the bed, is transferred to the particle No. 6, which travels in the upper region, via the particle No. 2 in the intermediate region with moderate height.

The interparticle collision, which plays a role of momentum transfer from the bottom region to the upper region, brings the change in the motion of individual particles. The particles traveling in an upper region of the bed-load layer are supplied with the upward vertical momentum by the collision with the ascending particles from the bottom region, to continue traveling in a long distance. While, the particles traveling in a bottom of the bed-load layer supply a portion of their upward vertical momentum to the particles traveling in the upper region, and their saltation lengths are assumed to be shorter due to the loss of the momentum.

### *Change in saltation trajectories*

Although the probabilistic variety exists in the individual saltation due to the irregular collision and repulsion at a bed surface, the interparticle collision brings the additional variety to the motion of

saltating particles. Fig. 9 shows some of the trajectories of the saltation with interparticle collision. The trajectories of the individual saltation are smooth in which the sudden change of the velocity and moving direction can be detected only in the collision and repulsion at the bed surface. While, the trajectories in Fig. 9 have many small notches with sharp edge, which indicate the sudden changes of velocity and moving direction of particle due to interparticle collisions.

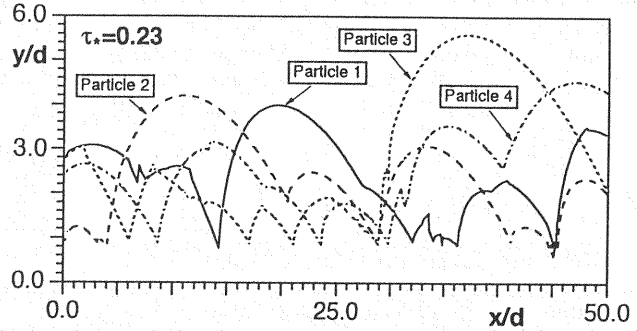


Fig. 9 Trajectories of saltation

#### Existing-probability distribution and velocity profile of saltating particles

To clarify the statistical characteristics of the saltation, the existing-probability distribution and mean-velocity profile of saltating particle are discussed. Fig. 10 shows the existing-probability distribution of saltating particles predicted by the present simulation (multiple-particle-tracing model; abbreviated as “MPT”-model) compared to that of single-particle-tracing model (abbreviated as “SPT”-model) and the experimental results. The experiment was conducted in open channel flow under the same condition as shown in Table 1. The motion of the particles were recorded by a CCD video camera through the transparent side walls of the flume. The existing-probability distribution and the velocity profile of saltating particles were investigated by analyzing the video film.

The SPT-model underestimates the existing probability in the upper region; but overestimates it in the middle region. While, the MPT-model shows an excellent agreement with the experiment in the whole region. The MPT-model can simulate the existence of the particle reaching the high region, to which a particle saltating independently of others (simulated by SPT-model) cannot attain, due to the interparticle collision. In other words, the particle moving in the upper region can continue traveling without touching the bottom surface by the provision of momentum due to the interparticle collision with the particles ascending from the lower region; and then, it reaches the higher region than the maximum height of saltation calculated by SPT-model.

Fig. 11 shows the velocity profile of saltating particle calculated by the present simulation (MPT-model) compared to that of SPT-model and the experimental results. Although, both of the MPT- and the SPT-model show the overestimation of the experimental result in the whole region, the MPT-model improves the discrepancy between SPT-model prediction and the experimental result. In detail, the experiment shows the change in the gradient of the profile in the middle region: the gradient in the upper region is steeper than that in the middle region, then the inflection point exists in the middle region. This tendency is fairly well predicted by the MPT-model. Fig. 12 shows the velocity profile of saltating particles normalized by the velocity at the height  $y/d=4.1$ . The defect of the bottom-neighboring velocity is well performed

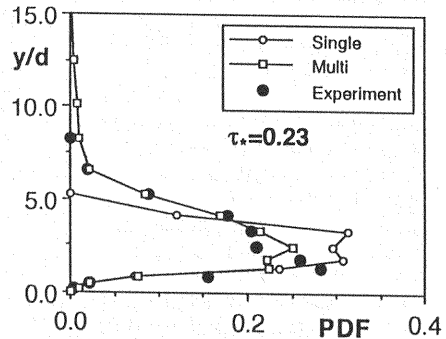


Fig. 10 Existing probability distribution of saltating particle

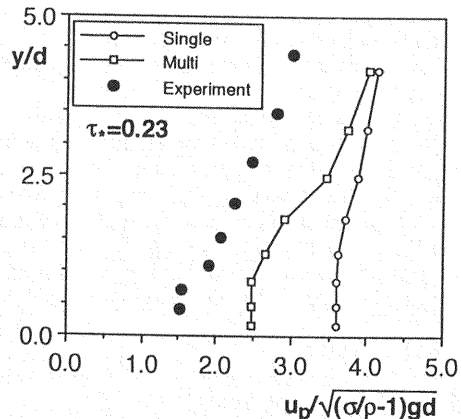


Fig. 11 Velocity profile of saltating particle



by the MPT-model, hence the important role of the interparticle collision on the bed-load transport in the bottom-neighboring layer is clarified.

Even the MPT-model cannot agree well quantitatively with the experiment. This can be regarded that the interphase momentum transfer, which brings the change in flow-velocity profile due to the existence of the saltating particle, is not considered in the present simulation. Fig. 13 shows the prediction of the two-phase flow model proposed by Nakagawa, Tsujimoto and Gotoh (6), in which the PSI (particle-source-in)-cell model is introduced to couple the  $k-\epsilon$  turbulence model of the flow with the Lagrangian model of saltation. The velocity profile in clear-water flow is attenuated by introducing the PSI-cell model for the interphase momentum transfer; but the whole shape of the velocity profile is not so much affected by the interphase momentum transfer. The combined model of the interphase and interparticle momentum transfer will bring the further improvement on the velocity profile of saltating particle.

## CONCLUSIONS

The two-dimensional simulation of the saltating particles in flowing water has been developed with special reference to the interparticle collision. The results obtained in this paper are summarized below:

(1) The series of snapshots of the present simulation express momentum transport in the upward vertical direction due to the interparticle collision.

(2) The trajectories of saltation are keenly affected by the interparticle collision: sudden change of the velocity and moving direction of saltating particle is brought by the interparticle collision.

(3) The existing probability distribution of saltating particles is estimated as a statistical characteristics of bed-load motion. The single-particle-tracing model underestimates the existing probability in the upper region, because it cannot consider the existence of the particle continuously moving in the upper region by the provision of the momentum due to the interparticle collision with the particle ascending from the lower region. The discrepancy between the experimental results and the single-particle-tracing model is modified by the present model.

(4) The velocity profile of the saltating particle, which is overestimated by the single-particle-tracing model in a whole region, is modified well by the present model. Change in the shape of the velocity profile, or the defect of the velocity in the bottom-neighboring region, is explained fairly well by the present model.

The constitution of the numerical model was already published in Japanese (14), but revised herein.

## ACKNOWLEDGMENT

The authors wish to express their gratitude to Mr. M. Watanabe (Graduate Students, Kyoto Univ.) for his help with the computer programming and data processing.

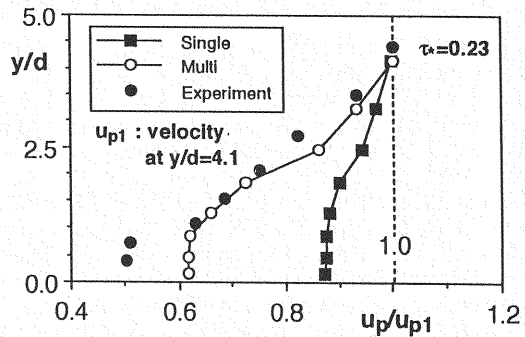


Fig. 12 Dimensionless velocity profile of saltating particle

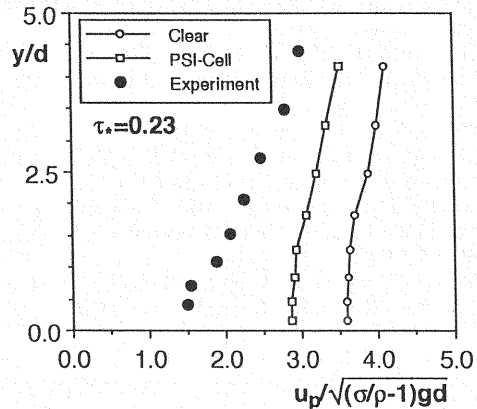


Fig. 13 Velocity profile of saltating particle (PSI-cell model for interphase momentum transfer)

## REFERENCES

1. Tsujimoto, T. and Nakagawa, H.: Stochastic Study on Successive Saltation by Flowing Water, *Proc. 2nd Int. Symp. on River Sedimentation*, Nanjing, China, pp. 187-201, 1983.
2. Tohdoh, M., Sekine, M. and Kikkawa, H.: Fundamental Study of Mechanism on Bed Load Movement, *Proc. the 27th Japanese Conf. on Hydraul.*, pp.299-304, 1983(in Japanese).
3. Wiberg, P. L. and Smith, D. J.: A theoretical model for saltating grains in water, *Jour. Geophys Res.*, 90(4), 7341-7354, 1987.
4. Sekine, M. and Kikkawa, H.: Mechanics of Saltating Grains, *Jour. Hydraulic Engrg.*, ASCE, Vol. 118, No.4, April, pp.536-558, 1992.
5. Crowe, C. T., Sharma, M. P. and Stock, D.E. :The Particle-Source-In Cell (PSI-CELL) Model for Gas-Droplet Flows, *Jour. Fluids Engrg.*, ASME, June, pp.325-332, 1977.
6. Nakagawa, H., Tsujimoto, T. and Gotoh, H.: Numerical simulation of bed-load layer as two-phase flow, *Int. Conf. Hydro-Sci. & Engrg.*, Washington D.C., USA, pp.638-645, 1993.
7. Cundall, P. A. and Strack, O. D.: A Discrete Numerical Model for Granular Assemblies, *Geotechnique*, Vol. 29, No. 1, pp.47-65, 1979.
8. Campbell, C. S. and Brennen, C. E.: Computer simulation of granular shear flows, *J. Fluid Mech.*, Vol. 151, pp.167-188, 1985.
9. Meguro, K., Iwashita, K. and Hakuno, M.: Fracture Analysis of Media Composed of Irregularly Shaped Regions by the Extend Distinct Element Method, *Structural Engrg. / Earthquake Engrg.*, JSCE, Vol. 8, No. 3, pp.131-142, 1991.
10. Rubey, W. W.: Settling Velocities of gravel, sand and silt, *American Jour. Science* Vol. 25, No.148, 1933.
11. Tsuchiya, Y. and Aoyama, T.: On the mechanism of saltation of a sand particle in a turbulent stream (2), *Annu. Disas. Prev. Res. Inst. Kyoto Univ.*, 13B, pp.199-216, 1970 (in Japanese).
12. Nakagawa, H., Tsujimoto, T. and Akao, T.: Stochastic Behaviors of Saltating Particles, *Proc. 27th Jap. Conf. Hydraul.*, JSCE, 1983 (in Japanese).
13. Meyer-Peter, E. and Müller, R.: Formula for Bed-Load Transport, *Proc. 2nd IAHR Cong.*, Stockholm, pp.39-64, 1948.
14. Gotoh, H., Tsujimoto, T. and Nakagawa, H.: Numerical Analysis of the Dynamics of Bed-Load Particles as Glandular Material, *Proc. Hydraul. Eng.*, JSCE, Vol. 37, pp. 611-616, 1993.

## APPENDIX-NOTATION

The following symbols are used in this paper:

$A_2, A_3$	= two-and three-dimensional geometrical coefficients of particle, respectively;
$C_D, C_{D\infty}$	= drag coefficients;
$C_M$	= added mass coefficient;
$d$	= diameter of particle;
$e, f$	= repulsive coefficients (=0.75);
$e_p, f_p$	= repulsive coefficients for interparticle collision (=0.8);
$g$	= gravitational acceleration;
$h$	= water depth;
$I_e$	= energy gradient;
$Re$	= Reynolds number;
$r_c$	= ratio of division between the position of particle at $t$ and $t+\Delta t$ ;
$U, V$	= mean flow velocity in streamwise and upward vertical direction, respectively;
$U_m$	= balk mean velocity;
$u_p, v_p$	= velocity of the saltating particle in streamwise and upward vertical direction, respectively;
$u_{gin}, v_{gin}$	= velocity of the saltating particle just before a collision in streamwise and upward vertical direction, respectively;

$u_{\text{gout}}, v_{\text{gout}}$	= velocity of the saltating particle just after a collision in streamwise and upward vertical direction, respectively;
$u_*$	= dimensionless shear velocity;
$x, y$	= coordinate in streamwise and upward vertical direction, respectively;
$x_i, y_i$	= coordinate of center of $i$ -th particle in streamwise and upward vertical direction, respectively;
$\alpha$	= angle of hypothetical repulsing plane against the mean bed surface;
$\Delta b$	= height of protruding obstruction on a bed;
$\Delta t$	= time step for calculation (=0.002 s);
$\theta_{\text{in}}$	= angle between depositing direction and the mean bed surface;
$\phi$	= angle of hypothetical repulsive plane against streamwise direction for the interparticle collision;
$\nu$	= kinematic viscosity;
$\rho$	= mass density of fluid;
$\sigma$	= mass density of particle; <i>and</i>
$\tau_*$	= dimensionless shear stress.

(Received July 20, 1994; revised November 30, 1995)